Langmuir

Article

pubs.acs.org/Langmuir

Dielectric Relaxation of Spherical Polyelectrolyte Brushes: Movement of Counterions and Electrical Properties of the Brush Layer

Haiyan Wu and Kongshuang Zhao*

College of Chemistry, Beijing Normal University, Beijing 100875, China

Supporting Information

ABSTRACT: Dielectric behaviors of spherical polyelectrolyte brush (SPB) suspensions under various mass fractions of SPB and the pH of solution were investigated in a frequency range of 40 Hz to 110 MHz. The SPB consists of a polystyrene (PS) core grafted with poly(acrylic acid) (PAA) chains. Two unique relaxations were found at either about 10 kHz or 1−10 MHz, respectively, with the former due to the diffusion of counterions and the latter resulting from the interfacial polarization. Using dielectric parameters of two relaxations, we obtained information about the migration of counterion and the conformation of polyelectrolyte chains. The PAA chains are fully stretched when pH is about 8 under the domination of the equilibrium between the penetration and diffusion of counterions in the brushes. A dielectric model is proposed to describe the high-frequency relaxation, and the permittivity and conductivity of SPB and its volume fraction were also calculated on the basis of the model. The surface conductivity of SPB, the Donnan potential, and the fixed charge density in the brush layer were derived from these paramaters. The distribution of the Donnan potential was also simulated by using Poisson−Boltzmann equations, and the result is in accordance with these obtained on the basis of the dielectric model.

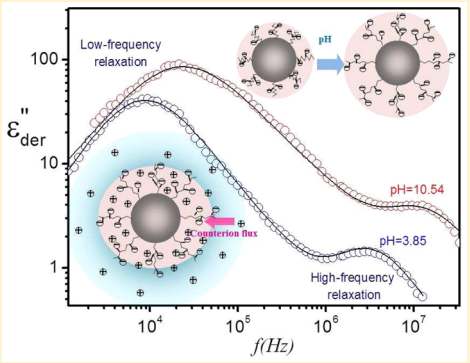

1. INTRODUCTION

Spherical polyelectrolyte brushes (SPBs) have attracted considerable attention since their synthesis by Ballauff et al. in 1999.[1] On the one hand, introducing charges through polyelectrolyte chains on the particle surface offers wide applications for SPBs as responsive biointerfaces, coatings, composite materials, and controlled drug-delivery and release systems.[2] On the other hand, it also created a model of a soft particle in which the core and bulk solution are separated by a brush layer. The model has been proven to play an important role in the stability of colloidal particles.[3] Recently, studies on the fundamental nature of SPBs have intensified.[4−6]

The wide applications of SPBs have been extensively reported in various fields. For example, the PS-PAA SPBs were used to synthesize Ag nanoparticles in situ for the SPB in order to improve its catalytic activity.[7] The thermosensitive PNIPAM network attached to the surface of the core particles has been reported to modulate the catalytic activity of Ag nanoparticles.[8] The studies on SPB mostly focus on the charge distribution[9] and the effect of solution conditions on the conformation of polyelectrolyte chains in the brush layer.[10−12] For a colloid particle, the surface charge can quantitatively generate repulsion energy between particles,[13] and the zeta potential on the particle surface can also impact the repulsive force and the stability of the whole suspension.[13,14] Long polyelectrolyte chains were grafted on the hard-core surface, and it becomes complex to assess the surface potential around the core. First, it is difficult to measure a reliable potential value from the electrophoretic mobility which is controlled by the valence, concentration, and distribution of counterions. More specifically, changing the charge of ions will lead to a significant collapse or spread of the chain, followed by the reduction of the zeta potential and decreased colloidal stability.[5,15] Moreover, such a shape change of the brush layer is also modulated by the pH of the solution.[12,16] To find out how the chain stretches are affected by the distribution, concentration, and kinds of counterions, many fundamental studies have been done. In fact, the morphology of the SPB brush is mainly determined by dynamic light scattering (DLS), which gives the overall dimensions of the particles in solution. Ballauff's group measured the hydrodynamic radius of SPB in varying polyelectrolyte chains using DLS and found that increases in ion concentration or a higher counterion valence led to a dramatic decrease in the zeta potential followed by the collapse of the SPB brush layer.[11−13] Cryogenic transmission electron microscopy (cryo-TEM) was ideally suited to study the structure of the polyelectrolyte surface layer.[17] On the other hand, the calculation method used to obtain the electrical parameters of the brush layer of SPB has been developed by Dukhin and Zimmermann.[18,19] They found that the surface conductivity at the grafted polyelectrolyte layer close to the bulk solution originated from the tangential movement of counterions, and the volume fixed charge density, an indication of the three-dimensional distribution of counterions, was

Received: April 17, 2015
Revised: June 19, 2015
Published: July 14, 2015

DOI: 10.1021/acs.langmuir.5b01408
Langmuir 2015, 31, 8566−8576

further estimated by combining with the Donnan potential and surface potential.

In addition, dielectric spectroscopy was also chosen to study the properties of the SPB suspension by Delgado and coauthors.[20] They found that the dielectric spectra of SPB suspensions displayed enormous loss peaks in the kHz frequency range, which was attributed to the dynamic mobility of SPB, and expounded that the huge dielectric increment was caused by the inhomogeneity of the counterion distribution in the brush layer.[21] Another advantage of studying SPB is that it has a well-defined core−shell structure, which is regarded as an exact model for soft particles. Ohshima reviewed a theory of the electrophoretic mobility of soft particles by focusing on the theoretical electrophoretic potential distribution and conductivity of the concentrated soft particles and proposed that all of these colloidal features are closely related to the dielectric properties of soft particles.[22] Recently, Cametti and colleagues studied the dielectric properties of other types of soft particles, such as ionic thiol-coated and PLGA-based nanoparticle suspensions.[23,24] Furthermore, he elaborated how the structure of the polymer soft layer might alter the dielectric response and the electrokinetic properties of the soft layer.[25]

It is well known that the dielectric theory of a typical particle dispersion was developed nearly half a century ago,[26] and has been successfully applied in many practical systems.[27] At present, the well-developed dielectric theories and models can give a good explanation of the relaxation behaviors of particle dispersions. In particular, the relaxation mechanisms at low and high frequencies have been established, attributed to surface diffusion[28] or volume diffusion for lower frequency[29] and interfacial polarization for higher frequency.[30] However, little is known about the dielectric relaxations of SPB caused by a polyelectrolyte brush, although Delgado et al. provide us an instructive example as mentioned above.

In conclusion, almost all studies on SPB agreed on the potential distribution in the brush layer and the effect of ion concentration on the zeta potential, while several questions remain unclear. Moreover, it is difficult to measure the exact charges inside brushes and define the true nature of the soft particle−solution interface.[25,31] Undoubtedly, the new work is expected to depict the electrokinetic properties of the spherical polyelectrolyte brush layer. In this article, dielectric spectroscopy of typical SPB which consists of polystyrene (PS) particles and grafted poly(acrylic acid) (PAA) is recorded as a function of the mass fractions of SPB and pH. We identified two specific dielectric relaxations displayed by SPBs, which are linked to the interpretation of the migration of the counterion inside the brush layer and the deformation of the layer. We analyzed the high-frequency relaxation in terms of interface polarization theory and calculated the electrical and structural parameters based on the Hanai equation. We also simulated the relationship between the potential and the charges in the brush layer based on Poisson's equation. Our study will be very helpful in understanding the impact of the dielectric properties of SPB on the movement of counterions around SPB and along the polyelectrolyte chains.

2. EXPERIMENTAL SECTION

2.1. Materials and Methods. *2.1.1. Materials.* Styrene (BASF) and acrylic acid (Fluka, AA) were distilled under reduced pressure to remove the inhibitor and stored at 4 °C before they were used. Potassium persulfate (KPS, Sigma-Aldrich) and sodium dodecyl sulfate (SDS, Sigma-Aldrich) were used without further purification. All reagents were analytical grade. Doubly distilled water was used in the experiment.

2.1.2. Synthesis and Characterization of the SPBs. The synthesis of the SPBs was perfomed according to the method developed by Xiang et al.[32] First, submicrometer monodisperse PS particles were prepared by emulsifer-free emulsion polymerization, and the radius of the PS core was determined to be 200 nm using dynamic light scattering (Peters ALV 4000). Second, HEMA was anchored on the surface of the above PS particles using "starve" addition, so hydroxyl is loaded on the particle surface, which induces it to form a stable suspension and proceed to the next step. Then the RAFT agent was anchored on the surface of the cross-linking PS particles through the Z group. The purpose of this step is to introduce the double bond on the particle surface through the esterification reaction between hydroxyl on the particle surface and carboxyl in the RAFT agent. In this way, functional monomers can be grafted onto the particle surface. Finally, functional monomers AA and photoinitiator were added, and pH-responsive brushes were obtained by UV-light-initiated surface polymerization. The radius of SPBs was determined to be 250 nm using DLS, indicating that the thickness of PAA was 50 nm. The specific preparation method has been reported elsewhere.[32]

2.1.3. Preparation of Samples. A series of different concentrations of SPB suspensions were prepared by adding a given volume of deionized water to a known mass fraction of an SPB suspension. The mass fraction ranges from 9.4 to 1.3%. The SPB suspensions with different pH values were adjusted by carefully adding a very small concentrated NaOH droplet to the suspensions to lower the ion concentration, and the pH (from 3.9 to 10.5) was monitored using a microprocessor pH meter. The dielectric spectrum for each SPBs suspension was measured directly after preparation.

2.2. Dielectric Measurements. Dielectric measurements (40 Hz to 110 MHz) of an SPB suspension were carried out using an HP4294A precision impedance analyzer from Agilent Technologies. A measurement cell (a detailed description is provided in the Supporting Information (SI)) with concentrically cylindrical platinum electrodes was employed and was described in detail in the previous work.[33] The applied electric field strength in the dielectric measurements is around 50 V m^{-1}, which is not capable of forming particle chains through dipole−dipole interaction. All measurements were carried out at room temperature (25 ± 0.5 °C). According to Schwan's lumped circuit method,[34] the experimental data errors arising from the terminal leads and measurement cell were corrected (see SI).

2.3. Determination of Dielectric Relaxation Parameters. Under the ac field, the complex permittivity of the SPB suspension is defined as

$$\varepsilon^*(\omega) = \varepsilon(\omega) - j\frac{\kappa(\omega)}{\varepsilon_0\omega} = \varepsilon(\omega) - j\left(\varepsilon''(\omega) + \frac{\kappa_l}{\omega\varepsilon_0}\right) \quad (1)$$

where $\varepsilon(\omega)$ and $\kappa(\omega)$ are the frequency-dependent real parts of the complex permittivity and conductivity, respectively, $\varepsilon''(\omega)$ is the frequency-dependent dielectric loss, κ_l is the low-frequency limit of conductivity, and $j^2 = -1$. The total dielectric loss contains two parts: the effective dielectric loss of the suspension and the low-frequency conductivity. The contribution of the low-frequency conductivity can be subtracted from the conductivity spectra through the equation

$$\varepsilon''(\omega) = \frac{(\kappa(\omega) - \kappa_l)}{\varepsilon_0\omega} \quad (2)$$

Accordingly, the following function including two Cole−Cole terms combined with an electrode polarization term $A\omega^{-m}$ (where A and m are adjustable parameters) was employed to analyze the experimental spectra[35] because two relaxations were observed in our measuring frequency window

$$\varepsilon^*(\omega) = \varepsilon_h + \frac{\Delta\varepsilon_{low}}{1 + (j\omega\tau_{low})^{\beta_1}} + \frac{\Delta\varepsilon_{high}}{1 + (j\omega\tau_{high})^{\beta_2}} + A\omega^{-m} \quad (3)$$

DOI: 10.1021/acs.langmuir.5b01408
Langmuir 2015, 31, 8566−8576

where $\Delta\varepsilon_{low} = \varepsilon_l - \varepsilon_m$ and $\Delta\varepsilon_{high} = \varepsilon_m - \varepsilon_h$ refer to low and high frequency dielectric increments, respectively, and β is the Cole−Cole parameter ($0 < \beta \leq 1$) indicating the distribution of relaxation times. Subscripts l, m, and h denote low-, medium-, and high-frequency limiting values, respectively. Here, high-frequency conductivity limits κ_h and medium-frequency conductivity limits κ_m were calculated through eqs 4a and 4b:[36]

$$\kappa_m = ((\varepsilon_l - \varepsilon_m)2\pi f_0 \varepsilon_0) + \kappa_l \quad (4a)$$

$$\kappa_h = ((\varepsilon_m - \varepsilon_h)2\pi f_0 \varepsilon_0) + \kappa_m \quad (4b)$$

Usually, the electrode polarization (EP) perturbs the measurement especially for the solution systems with higher ion concentration. The EP effect leads to the absence of a clear low-frequency plateau in the permittivity as shown in the inset of Figure 1. Many methods or technologies are used to correct the EP effect. Serghei et al.[37] described a detailed analysis of the dielectric data of EP based on the charge-transport mechanism at an ion−metal interface. We used the logarithmic derivative method[27,38,39] based on the following derivative to optimize the fitting and determine the characteristic frequency

$$\varepsilon''_{der}(\omega) = -\frac{\pi}{2}\frac{\partial\varepsilon}{\partial \ln \omega} \approx \varepsilon''_{rel}(\omega) \quad (5)$$

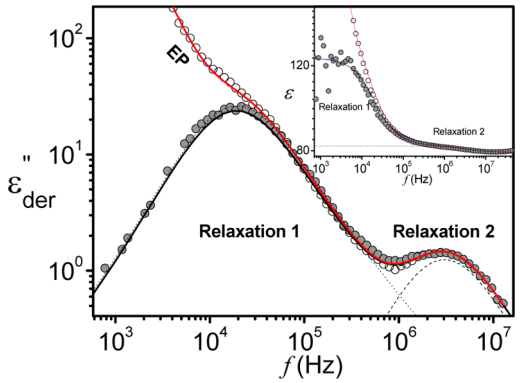

Figure 1. Frequency dependence of derivative dielectric loss $\varepsilon''_{der}(\omega)$ (hollow circles) and corrected data after subtraction of the EP effect (solid circles) of pH 3.85 for an SPB mass fraction of wt = 0.536% at a salt concentration ca. 10^{-4} mol/L: red solid line, best fit with EP; black solid line, best fit without EP; dotted line, low-frequency relaxation; dashed line, high-frequency relaxation. The inset shows the fitting result of the relative permittivity ε by using the same fitting parameters.

where $\varepsilon''_{der}(\omega)$ and $\varepsilon''_{rel}(\omega)$ denote the derivative dielectric loss based on the logarithmic derivative and the dielectric loss free of dc conductivity, respectively. This method has been proven to be effective in separate relaxations from the EP effect and also offers a good way to resolve overlapping relaxation peaks due to peak sharpening.[36] By introducing the real part of eq 3 into eq 5, we derived the expressions

$$\varepsilon''_{der}(\omega) = \frac{\pi}{2}\left(\sum_i \frac{\beta_i(\Delta\varepsilon_i)(\omega\tau_1)^{\beta_i}\cos\left[\frac{\beta_i\pi}{2} - (1+\beta_i)\theta_i\right]}{1 + 2(\omega\tau_i)^{\beta_i}\cos\frac{\beta_i\pi}{2} + (\omega\tau_i)^{2\beta_i}}\right) \quad (6a)$$

$$\theta_i = \arctan\left[\frac{\sin\left(\frac{\beta_i\pi}{2}\right)}{(\omega\tau_i)^{\beta_i} + \cos\left(\frac{\beta_i\pi}{2}\right)}\right] \quad (6b)$$

The two equations have the same set of variables as those in eq 3 and can be used to fit the derivative dielectric loss spectra. First, the raw permittivity data were fitted using eq 3, by which the values of A and m were determined. The EP effect was then subtracted from the raw permittivity data at every frequency by use of A and m. Then, the new permittivity ε was transferred into ε''_{der} using eq 5 (solid circles in Figure 1). The relaxation parameters were determined by fitting eq (6) to $\varepsilon''_{der} \approx f$ data.

Figure 1 represents an example of the frequency dependence of $\varepsilon''_{der}(\omega)$ (hollow circles) of pH 3.85 of a 0.536% SPB suspension and the result after the subtraction of the EP effect (solid circles). The solid black line is the best fitting by eq 6. The inset of Figure 1 shows the frequency dependency of ε (hollow circles) and that after subtraction of the EP (solid circles). The solid black line is the result calculated by use of the relaxation parameters obtained from fitting the $\varepsilon''_{der}(\omega) \approx f$ curve. Figure 1 shows the good agreement between the calculation and the data after subtracting EP, indicating the appropriate application of the logarithmic derivative method to our data.

3. RELEVANT MODEL AND THEORY

3.1. Dielectric Model of the SPB Suspension and Hanai Equations. Spherical polyelectrolyte brushes (SPBs) in this study can be depicted as in Figure 2(b), where R and L are the radii of the PS core and the thickness of the polyelectrolyte layer, respectively. The fixed charge in the polyelectrolyte layer is $-COO^-$, and the counterion is H^+. Figure 2(a) shows the schematic of the SPB suspension: the SPB particles with radius R_b (= R + L) and complex permittivity ε^*_{SPB} are dispersed in a continuous media of permittivity ε^*_a in a volume fraction ϕ.

On the basis of the model, the following Hanai equation[40] can appropriately describe the present SPBs suspension

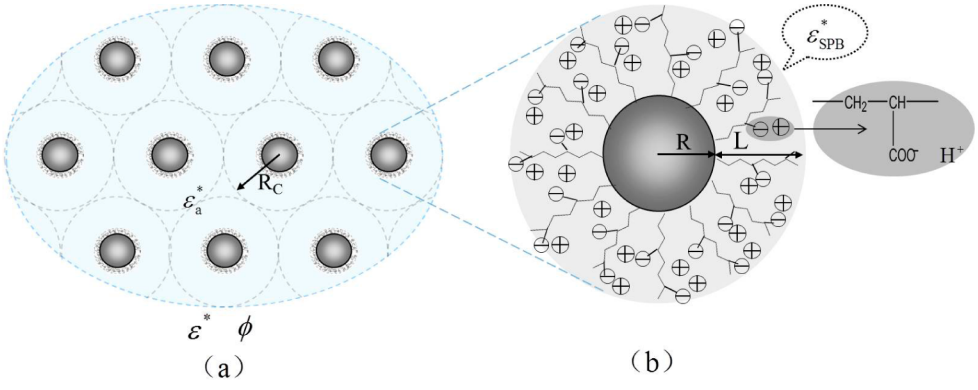

Figure 2. (a) Schematic of SPB suspension consisting of a PS core and a PAA polyelectrolyte chain as well as the schematic sketch according to the Kuwabara cell model. R_c is the radius of Kuwabara's cell, ε^* and ε^*_a are the complex permittivities of SPB suspensions and continuous media, and ϕ is the volume fraction of SPBs in the suspension. (b) A single SPB, where R is the radius of the PS core and L is the thickness of the PAA polyelectrolyte chain. ⊕, H^+; ⊖, $-COO^-$. ε^*_{SPB} is the complex permittivity of SPB.

DOI: 10.1021/acs.langmuir.5b01408
Langmuir 2015, 31, 8566−8576

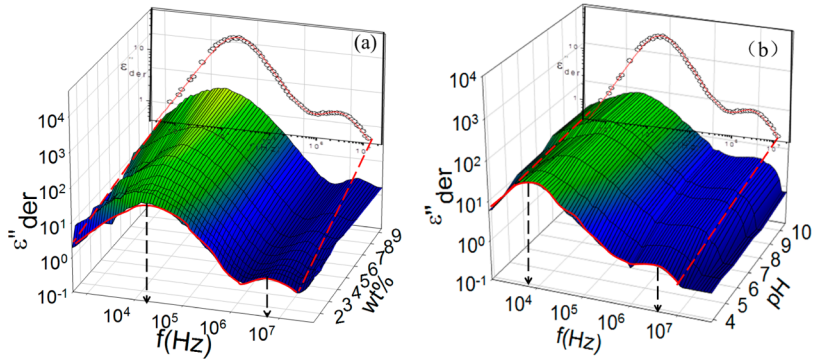

Figure 3. Three-dimensional representations of mass fraction dependence of the derivative dielectric loss spectra (a) and pH dependence of the dielectric loss when the mass fraction is 0.536% (b) for a salt concentration range of 10^{-4}−10^{-5} mol/L. They have been processed by eliminating the electrode polarization. The arrows indicate the low and high relaxation frequencies. The inset is the best-fitting curve fitted by eq 6.

Table 1. Relaxation Parameters for SPBs Suspensions of Different Mass Fractions (a) and Different pH Values of 0.536% SPBs (b)

(a)	wt %	ε_l	ε_m	ε_h	$\Delta\varepsilon_{low}$	$\Delta\varepsilon_{high}$	$\tau_{low}/\mu s$	τ_{high}/ns	β_{low}	β_{high}
	1.3	163.3 ± 4	81.5 ± 2	80.02 ± 0.3	81.8	1.48	4.44 ± 0.09	24.30.9	0.9620.08	1
	1.6	178.3 ± 5	81.5 ± 2	79.95 ± 0.3	96.8	1.55	4.37 ± 0.09	21.20.8	0.9530.07	1
	1.8	185.3 ± 4	80.6 ± 3	78.72 ± 0.2	104.7	1.55	4.14 ± 0.07	18.90.8	0.9630.05	1
	2.1	208.5 ± 5	80.3 ± 1	78.33 ± 0.4	128.2	1.97	4.06 ± 0.08	17.50.7	0.9640.05	1
	2.5	235.5 ± 5	80.0 ± 2	77.99 ± 0.5	155.5	2.01	3.99 ± 0.07	16.80.8	0.9640.06	1
	3.1	250.5 ± 6	80.4 ± 3	77.98 ± 0.4	170.1	2.42	3.91 ± 0.07	15.10.8	0.9630.05	1
	3.8	269.3 ± 6	79.3 ± 3	76.98 ± 0.3	190.0	2.32	3.64 ± 0.08	12.70.6	0.9550.06	1
	4.7	281.5 ± 7	78.4 ± 2	75.92 ± 0.3	203.1	2.48	3.54 ± 0.09	12.20.6	0.9570.06	1
	6.2	297.5 ± 8	76.0 ± 1	73.33 ± 0.5	221.5	2.67	2.81 ± 0.08	11.80.7	0.9710.05	1
	9.4	305.5 ± 8	74.0 ± 3	71.25 ± 0.4	231.5	2.75	2.65 ± 0.07	10.90.7	0.9700.05	1
(b)	pH	ε_l	ε_m	ε_h	$\Delta\varepsilon_{low}$	$\Delta\varepsilon_{high}$	$\tau_{low}/\mu s$	τ_{high}/ns	β_{low}	β_{high}
	3.9	122.6 ± 2	82.9 ± 2	80.92 ± 0.3	39.7	2.61	8.72 ± 0.5	51.7 ± 1.0	0.893 ± 0.07	0.923 ± 0.08
	4.7	132.6 ± 7	83.7 ± 2	80.94 ± 0.3	48.9	2.76	6.24 ± 0.3	39.6 ± 0.8	0.832 ± 0.05	0.903 ± 0.08
	5.7	147.7 ± 6	85.6 ± 4	81.00 ± 0.3	62.1	4.60	4.55 ± 0.2	26.3 ± 0.6	0.842 ± 0.04	0.884 ± 0.07
	6.7	174.1 ± 5	88.3 ± 3	81.09 ± 0.4	85.8	7.21	4.35 ± 0.3	18.8 ± 0.4	0.852 ± 0.06	0.794 ± 0.08
	7.4	184.1 ± 8	88.3 ± 4	80.25 ± 0.3	95.8	8.05	4.34 ± 0.3	16.2 ± 0.4	0.834 ± 0.05	0.771 ± 0.05
	8.1	188.1 ± 8	90.4 ± 5	82.30 ± 0.4	97.7	8.10	3.92 ± 0.2	13.8 ± 0.3	0.827 ± 0.04	0.791 ± 0.05
	10.5	198.1 ± 7	89.1 ± 5	83.39 ± 0.5	109	5.71	3.08 ± 0.2	13.3 ± 0.3	0.807 ± 0.03	0.851 ± 0.04

$$\frac{\varepsilon^* - \varepsilon^*_{SPB}}{\varepsilon^*_a - \varepsilon^*_{SPB}}\left(\frac{\varepsilon^*_a}{\varepsilon^*}\right)^{1/3} = 1 - \phi \tag{7}$$

where $\varepsilon^*_{SPB} = \varepsilon_{SPB} - j\kappa_{SPB}/\omega\varepsilon_0$ and $\varepsilon^*_a = \varepsilon_a - j\kappa_a/\omega\varepsilon_0$. The electrical parameters of SPB and the medium, i.e., phase parameters named in this work (ϕ, ε_{SPB}, κ_{SPB}, and κ_a) are related to the relaxation parameters of the dielectric measurement (ε_m, ε_h, κ_m, and κ_h):

$$\varepsilon_m\left(\frac{3}{\kappa_m - \kappa_{SPB}} - \frac{1}{\kappa_m}\right) = 3\left(\frac{\varepsilon_a - \varepsilon_{SPB}}{\kappa_a - \kappa_{SPB}} + \frac{\varepsilon_{SPB}}{\kappa_m - \kappa_{SPB}}\right) - \frac{\varepsilon_a}{\kappa_a} \tag{8}$$

$$\kappa_h\left(\frac{3}{\varepsilon_h - \varepsilon_{SPB}} - \frac{1}{\varepsilon_h}\right) = 3\left(\frac{\kappa_a - \kappa_m}{\varepsilon_a - \varepsilon_{SPB}} + \frac{\kappa_m}{\varepsilon_h - \varepsilon_{SPB}}\right) - \frac{\kappa_a}{\varepsilon_a} \tag{9}$$

$$\frac{\kappa_m - \kappa_{SPB}}{\kappa_a - \kappa_{SPB}}\left(\frac{\kappa_a}{\kappa_m}\right)^{1/3} = 1 - \phi \tag{10}$$

The phase parameters can be calculated from the relaxation parameters using eqs 8−10 by a systematic numerical method[41] if the permittivity of the medium solution, ε_a, is given.

3.2. Cell Model. Kuwabara's cell model[41] is frequently used to describe a concentrated suspension. According to the cell model, each individual particle (e.g., a soft particle consists of the particle core of radius R covered with a polyelectrolyte layer of thickness L) in a dispersed system is considered to be a cell with a radius of $R_b = R + L$. In other words, it is thought that each soft particle can be regarded as being surrounded by a concentric spherical shell of an electrolyte solution with an outer radius of R_c (Figure 2(a)). Hence, the particle/cell volume ratio in the unit cell is equal to the particle volume fraction ϕ throughout the entire suspension via

$$\phi = \left(\frac{R_b}{R_c}\right)^3 \tag{11}$$

It is worth noting that ϕ in Kuwabara's cell model has the same value as ϕ in the Hanai equation.

DOI: 10.1021/acs.langmuir.5b01408
Langmuir 2015, 31, 8566−8576

4. RESULTS AND DISCUSSION

4.1. Dependency of Relaxation Parameters on Mass Fraction and pH. After the elimination of electrode polarization according to the equations in section 2.3, the derivative dielectric loss spectra of SPB suspensions were shown over a frequency range from 40 Hz to 110 MHz either in a mass-fraction-dependent way (Figure 3(a)) or in a pH-dependent way (Figure 3(b)). Two dielectric relaxations were found at around 10^4 Hz and 10^7 Hz, which were well fitted by eq 6 as shown in the inset of Figure 3. We derived various relaxation parameters of SPBs of different mass fraction in the pH range of 4−10 based on the dielectric model described in section 3 (Table 1).

Both $\Delta\varepsilon_{low}$ and $\Delta\varepsilon_{high}$ increased with either the increasing mass fraction of SPBs or the increasing pH of the solution, with a larger value of $\Delta\varepsilon_{low}$ compared to that of $\Delta\varepsilon_{high}$ (Table. 1). On the other hand, τ_{low} and τ_{high} decreased when the mass fraction of SPB and the pH of the solution increased. We also found that the distribution parameters at low and high frequencies of the two relaxations, β_{low} and β_{high}, were different. For the suspensions of varying mass fraction, β_{low} and β_{high} were very close to 1, implying the homogeneity of structural and electrical properties of brushes layer of SPB. As for the pH, β_{low} and β_{high} were in the range of 0.9−0.8, which might reflect the heterogeneity of brush layers and the change in the interfacial property. The heterogeneity possibly originated from the nonuniform distribution of segment density and charge density in the PAA brush, where a dense layer of larger charge density was close to the core but a sparse layer of smaller charge density was far away from the core. In general, the ionic polarization on the order of kHz and interfacial polarization at higher frequency was considered to be less responsible for the relaxation behavior displayed by the particle suspension.[27] Therefore, some valuable information about the particles and the solution in suspension can be obtained by analyzing the high-frequency relaxation, and on this basis the electrical properties of the electric double layer (EDL) and the brush layer around the particle can be estimated by identifying the mechanism of low-frequency relaxation.[42,43]

4.2. Migration of Counterions in the Brush Layer. *4.2.1. Low-Frequency Relaxation Mechanism: Counterion Diffusion.* For a conventional hard particle, low-frequency relaxation is caused by the tangential or longitudinal motion of the counterion around the particle, called the counterion polarization. Under the electric field the ion concentration gradient in EDL gives rise to a unsymmetrical distribution, and the ions recover a symmetrical distribution by diffusion when the electric field disappears. The time for the counterions to recover the equilibrium distribution was related to the concentration of the solution and the construction of the EDL.[27] However, for SPB, the existing EDL around the hard particle was replaced by a permeable and charged polyelectrolyte chain layer.[25,44] Therefore, the low-frequency dielectric relaxation might consist of more than one polarization mode.

In this study, given that the acrylic acid of polyelectrolyte brush was partially ionized, the fixed charges could be carboxyl groups on a polyelectrolyte chain, while the hydrogen ion served as the counterion. According to the strength of their interaction with the fixed charges, the counterions could be divided into condensed counterions and free counterions. Hence, most of the condensed counterions were trapped in the brush layer, while the free counterions can go inside the brush layer relatively freely under the effect of the Donnan potential.

Delgado et al. found that the low-frequency relaxation was caused by counterion exchange between the polyelectrolyte brush and the bulk, i.e., the diffusion of counterions driven by the concentration gradient.[29] Theoretically, when the polyelectrolyte chains are fully stretched, the fixed charges are equally distributed along the chain with the identical potential inside the chain layer, and the distribution of counterion resembles the EDL with the existence of the diffusion layer in the boundary between SPB and the bulk solution. The potential distribution and counterion distribution could be expressed by Poisson's equation.[45,46] For the particular case of a planar soft interface (equivalently, $R \gg L$), Ohshima simplified Poisson's equation in the symmetrical valence electrolyte:[22]

$$\frac{d^2}{dr^2}\psi = \begin{cases} -\sum_{j=1}^{N} \frac{ez_j n_j}{\varepsilon_m \varepsilon_0} - \frac{\rho_{fix}}{\varepsilon_m \varepsilon_0} & \text{if } R < r < R + L \\ -\sum_{j=1}^{N} \frac{ez_j n_j}{\varepsilon_m \varepsilon_0} & \text{if } r > R + L \end{cases} \tag{12a}$$

$$n_j(r) = n_j(\infty)\exp\left(-\frac{z_j e\psi}{k_B T}\right) \tag{12b}$$

Figure 4 shows the simulation of the potential distribution and counterion distribution around the SPB using eq 12. The

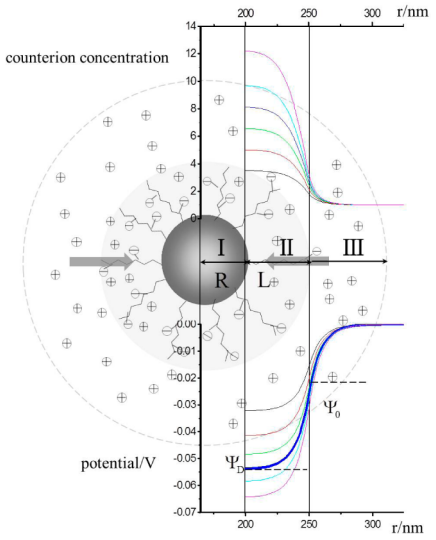

Figure 4. Equilibrium potential distribution around SPB particles simulated by using the following parameters: core radius R = 200 nm, polyelectrolyte thickness L = 50 nm with $Q = 1 \times 10^{-14}$−3.8×10^{-14} C (bottom to top), ionic strength 1 mM KCl, and volume fraction ϕ = 0.08.

potential distribution along the radius direction of SPB is found to be consistent with that of the counterion concentration distribution, which is in accordance with the literature.[47] When an ac field is applied to the charged SPB particles, the diffusion of counterion H^+ (as indicated by the arrow in Figure 4) driven by the concentration gradient leads to ion polarization of two sides of the particle, leading to low-frequency relaxation derived from the volume diffusion of free counterions.[20] On the other hand, potential distribution zone II in Figure 4 is related to the

DOI: 10.1021/acs.langmuir.5b01408
Langmuir 2015, 31, 8566−8576

Donnan potential determined by the fixed charge density, and it can be obtained by analyzing the high-frequency relaxation later. In addition, zone III is an extension of the polyelectrolyte brush zone, similar to the diffuse layer of EDL in a hard particle.

According to volume diffusion theory established by Delgado et al.,[29] the relaxation time τ_{theory} of the low-frequency relaxation is controlled by the characteristic distance L_D. The relationship between τ_{low} and L_D can be described by Einstein's equation:

$$\tau_{theory} = {L_D}^2/D_{H^+} \quad (13)$$

Here, D_H is 9.311 × 10^{-9} m^2s^{-1} according to ref 47. In the moderately concentrated suspension, L_D could be defined as

$$L_D = R\left(1 + \frac{1}{(\phi^{-1/3} - 1)^2}\right)^{-1/2} \quad (14)$$

where ϕ (= $(R_b/R_c)^3$; the meanings of R_b and R_c are depicted in Figure 2) is the volume fraction of SPBs in suspension and can be calculated from eqs 8−10 which will be discussed in later sections. According to eqs 13 and 14, τ_{theory} and L_D were calculated and summarized in Table 2, as were the values of τ_{low} in Tables 1 and 2.

Table 2. Characteristic Distance L_D and Relaxation Time τ_{theory} of Different Mass Fractions of SPBs (a) and Different pH Values of 0.536% SPBs (b) Based on Volume Diffusion Theory

(a)	wt %	L_D/nm	$\tau_{theory}/\mu s$	$\tau_{low}/\mu s$
	1.3	143	2.21	4.44
	1.6	133	1.91	4.37
	1.8	126	1.71	4.14
	2.1	118	1.50	4.06
	2.5	107	1.23	3.99
	3.1	85	0.779	3.91
	3.8	72	0.565	3.64
	4.7	62	0.414	3.54
	6.2	45	0.224	2.81
	9.4	35	0.132	2.65
(b)	pH	L_D/nm	$\tau_{theory}/\mu s$	$\tau_{low}/\mu s$
	3.9	154	2.57	8.72
	4.7	151	2.45	6.24
	5.7	148	2.37	4.55
	6.7	142	2.17	4.35
	7.4	136	1.98	4.34
	8.1	130	1.81	3.92
	10.5	130	1.81	3.08

We found that the calculated relaxation times τ_{theory} of the two systems decreased as either the mass fraction of SPBs, i.e., volume fraction, or the pH of the medium. The possible reason is that as the mass fraction increases, the distance (L_D) between the SPBs is equivalently shortened, leading to decreased τ_{theory} based on eq 13. On the other hand, on the basis of eq 14, increasing pH means increasing the degree of ionization, which leads to the increasing repulsive interaction between PAA chains, resulting in the increase in both the radius and volume fraction of SPBs. Although the calculated values are smaller than that from dielectric observation, they are comparable in order of magnitude. The error might derive from the volume fraction in the model which contains the polyelectrolyte layer.

4.2.2. Specific Low-Frequency Dielectric Increment. On the basis of the above discussion, we confirmed that the low-frequency relaxation was caused by the volume diffusion of free counterions, hence the dielectric increment is considered to be related to the charge distribution and the thickness. The values of the dielectric increment are about 80−230 for the case of the mass fraction change and about 40−110 for the case of the pH change (Table 1), which are similar to that of bare particles,[48,49] partially because of the assumption that the radius R was much larger than L in this work. If L were much larger than R, then there would be a giant dielectric increment at low frequency as was reported by Delgado, who found the strong dielectric relaxation behavior at low frequency for the SPB suspension.[20]

We studied the correlation of the specific dielectric increment ($\delta\varepsilon_l = (\varepsilon_l - \varepsilon_m)/wt$) of the low-frequency relaxation with either the mass fraction of SPBs (Figure 5(a)) or the pH

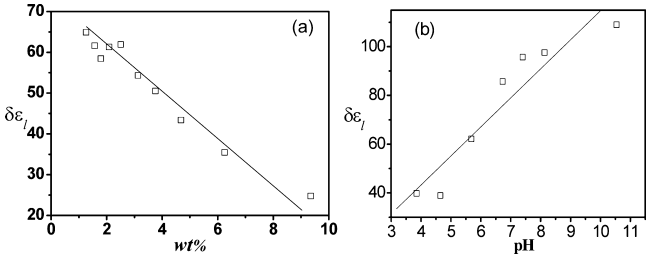

Figure 5. Mass fraction dependence of the specific dielectric increment (a) and the pH dependence of the specific dielectric increment when the mass fraction of SPBs is 0.536% (b).

of the solution (Figure 5(b)). The specific dielectric increment $\delta\varepsilon_l$ was inversely proportional to the mass fraction (Figure 5(a)), being coincident with the prediction of volume diffusion theory.[29] In contrast, $\delta\varepsilon_l$ increased as the pH of the solution increased (Figure 5(b)), which is opposite to the trend observed for the mass fraction of SPBs. This phenomenon suggests that the degree of ionization increases as the pH of the solution increases, and the increasing fixed charge density of carboxylic acid in PAA chains allows more counterions to permeate the brush layer, leading to the rise of the Donnan potential. As a result, the increasing concentration gradient between the brush layer and the bulk solution enhanced the diffusion migration of counterions from the bulk to the brush layer, leading to the increase in $\delta\varepsilon_l$.

4.2.3. Fluctuation of Counterions in the Brush Layer. We found a distinct dielectric relaxation at about 10 MHz for both suspensions (Figure 2). In fact, the diffusion of free counterions to the brush layer of SPB can generate a low-frequency relaxation as mentioned above. In addition, the mobility fluctuation of the condensed counterion along the polyelectrolyte chain was found to contribute to dielectric relaxation, which is generally observed at a higher frequency range of about 1−10 MHz.[50] According to Einstein's equation,[51] the relaxation time is expressed as

$$\tau_{high} = {R_s}^2/2D'_{H^+} \quad (15)$$

where D'_{H^+} is the diffusion coefficient of H^+ along the polyelectrolyte chain, which is reduced by a factor of 1.5 in the soft layer[20,52] compared to D_{H^+} (= 9.311 × 10^{-9} s^{-1}) in solution as mentioned above. R_s is the distance of the condensed counterion fluctuation along the chain. Using eq 15, R_s is calculated using τ_{high}. The values of R_s ranged from 17

DOI: 10.1021/acs.langmuir.5b01408
Langmuir 2015, 31, 8566−8576

to 11 nm when the mass fraction of SPBs varied from 1.3 to 9.4%, while they decreased from about 25 to 13 nm when the pH of the solution increased from 3.9 to 10.5.

The space occupied by an individual SPB particle decreases as the mass fraction of SPB increases, which leads to the collapse of polyelectrolyte chains, i.e., the folding of PAA chains. Although the amount of fixed charge is unchanged, the position of fixed charge changes in PAA chains and the distance between the fixed charges in the PAA layer decreases. As a result, the distance of the counterion fluctuation decreases because the length of the subunit is shortened.[53] And when the pH increases, more −COOH on PAA chains are ionized and the amounts of fixed charge $COOH^-$ on the chains increase correspondingly, which resulted in a decrease in the distance between fixed charges. Consequently, the high-frequency relaxation time obviously decreases with the increase in the pH of the solution.

Our results support the assumption[54] that the fluctuation of counterions along the polyelectrolyte chain contributes to high-frequency relaxation. Moreover, our result implies that the PAA chain is not fully stretched in certain ranges of SBP mass fractions, which is expatiated in the next section.

4.3. Stretch and Collapse of Polyelectrolyte Brushes. *4.3.1. Dielectric Analysis Model of High-Frequency Relaxation.* By means of the dielectric model and analysis method introduced in section 3.1, we calcualted phase parameters by using eqs 8−10 from the dielectric parameters (ε_l, ε_m, ε_h, κ_m, κ_h, and ε_a) listed in Table 1. The calculated phase parameters are listed in Table 3 for either SPB suspensions of different mass

Table 3. Phase Parameters Calculated for SPB Suspensions of Different Mass Fractions (a) and for 0.536% SPB Suspensions of Varying pH (b) from the Dielectric Parameters Listed in Table 1 Using Equations 8−10

(a)	wt %	ϕ	ε_{SPB}	κ_{SPB}/S m^{-1}	κ_a/S m^{-1}
	1.3	0.2036	86.34	0.02171	0.0116
	1.6	0.2307	85.07	0.02465	0.0134
	1.8	0.2515	79.51	0.02608	0.0145
	2.1	0.2753	78.00	0.02805	0.0160
	2.5	0.3114	76.96	0.03056	0.0178
	3.1	0.3954	77.25	0.03377	0.0193
	3.8	0.4517	75.21	0.03609	0.0214
	4.7	0.5041	75.54	0.04043	0.0240
	6.2	0.5996	70.03	0.04754	0.0286
	9.4	0.6720	67.90	0.05161	0.0308

(b)	pH	ϕ	L/nm	ε_{SPB}	κ_{SPB}/S m^{-1}	κ_a/S m^{-1}
	3.9	0.1749	50.0	93.29	0.01242	0.005606
	4.7	0.1838	54.2	92.62	0.01631	0.006677
	5.7	0.1897	56.9	92.51	0.02878	0.009886
	6.7	0.2068	64.4	91.75	0.03974	0.01148
	7.4	0.2239	71.5	86.68	0.04361	0.01280
	8.1	0.2402	77.9	95.316	0.04778	0.01352
	10.5	0.2397	77.7	100.46	0.06519	0.02098

fractions (Table 3(a)) or 0.536% SPBs suspensions of varying pH (Figure 3(b)). It is clearly shown that the length of the PAA chains, i.e., the thickness of brush layer L calculated from ϕ, was controlled by the pH of the solution (Figure 3(b)).

The conductivity of SPB, κ_{SPB}, is found to be several times larger than that of bulk κ_a, and both of them increased as the SPB mass fraction of the SPB suspension and the pH of the solution increased, directly reflecting the existence of highly concentrated counterions in the polyelectrolyte brush layer[53] (zone II in Figure 4). The motion of the counterions is a direct consequence of the increase in κ_{SPB}. From the microscopic view, when SPB particles are added to suspension, dynamic deformation of PAA chains leads to the collapse of the brush layer and increases the fixed charge density, resulting in the trap of more counterions in the brush layer. While the pH of the solution increases, more and more −COOHs on the PAA chains are neutralized and cause an increase in the number of charge sites ($-COO^-$) on the PAA chains. Consequently, a larger number of counterions penetrate the brush layer, and the additional counterion fluctuation along the PAA chains gives rise to a larger conductivity.[18]

The permittivity ε_{SPB} of SPB with varying mass fraction shows a value close to the permittivity of pure water (ε_a = 78.35, 25 °C) and a value larger than the pure water permittivity for varying pH, which might relate to the hydrogen bond between a water molecule and a polyelectrolyte chain. In general, the water content in the polyelectrolyte is approximate to 95%, and it increases when the swelling of the polyelectrolyte brushes occurs. Therefore, it is acceptable that the value of ε_{SPB} approaches that of water. Furthermore, the hydrogen-bond interaction was found between the water molecule and the carboxyl group on the chains[55] and organized a confined space as depicted in Figure 6(a). In the space, the ordered array of

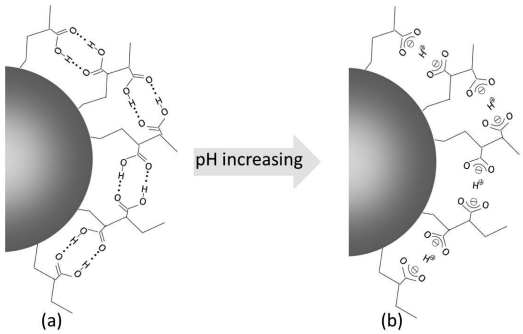

Figure 6. (a) When the pH is lower, a confined space is formed by the hydrogen-bonding interaction between carboxyl and the carboxyl group on the PAA chain. (b) When the pH is higher, a continuous conductive structure is constructed by carbonyl group and H^+.

water molecules forms an apparent dipole, resulting in an additional permittivity because of the reorientation under the ac electric field. On the other hand, with increasing pH, more and more carboxyl groups (−COOH) were turned into carbonyl groups ($-COO^-$) and led to formation of a construction as shown in Figure 6(b). The $-COO^-$ charge sites are continuously arranged on the skeleton of the PAA chain, and the condensed counterions along the PAA chain constitute a continuous electrically conductive structure. In other words, a series of small dipoles form between the carbonyl group ($-COO^-$) and H^+, which accumulates a huge apparent dipole and also contributes to the apparent permittivity of the SPB particle.[56]

4.3.2. Stretching and Collapse of PAA Brushes. The volume fraction calculated from the high-frequency relaxation increases with the SPB mass fraction and pH of the solution (Table 3). Under a given volume, the increase in mass fraction means an increasing number of SPBs in suspension. According to the cell model, R_c decreased when ϕ increased, indicating that the thickness L is compressed and became thinner because of the

DOI: 10.1021/acs.langmuir.5b01408
Langmuir 2015, 31, 8566−8576

interaction between SPBs particles[17] or L remained unchanged but the medium space $(R_c - (R + L))$ decreased. Our results showed the possibility of the latter; at least the compression of the medium space $(R_c - (R + L))$ is larger than that of the polyelectrolyte brush because of the increasing number of SPB particles. It is inevitable because we indeed added the SPB particles in the experiment for the case of varying SPB mass fraction. However, it is interestingly found that the calculated volume fraction ϕ also increased as the pH of the solution increased at a given mass fraction of 0.536% for SPB. It is clear that R_c was kept unchanged because of the constant number of SPBs at a certain mass fraction of 0.536%. Therefore, the result suggests that at lower pH, most of the carboxylic acid groups −COOH in the PAA chain are undissociated, leading to the slight stretching of the PAA chain because of the interaction between adjacent chains; as the pH increases, the degree of dissociation of −COOH and the fixed charge density increase, resulting in an increase in the electrostatic repulsion between chains until the chains are fully outstretched. On the other hand, the increasing fixed charge density also caused the osmotic pressure of the brush layer, which facilitated the permeation of more hydrated counterions into the brush layer, resulting in swelling. The two effects possibly made L thickened and $(R + L)$ increased (Table 3(b)).

In general, for the SPB suspension, it is hard to confirm the nature of the true interface between the SPB particle and the outer electrolyte solution. Therefore, analyzing dielectric spectra theoretically become more difficult.[25] In this sense, the analysis results listed in Table 3 become especially important. The discussions above suggest that the exact boundary between a soft particle and the external medium may be located at the junction of the soft layer and the solution.

4.4. Electrical Parameter of the Polyelectrolyte Brush and the Interface. It is generally known that the structure and the resulting function of polyelectrolyte brushes depend on the degree of ionization of the polyelectrolyte and the surface charges characterized by the Donnan potential which directly decides the electrostatic stabilization of the colloidal particle.[13] In addition, surface conductivity is directly related to the electrokinetic property of SPBs because it provides information about the number of ions and their distribution.[57] According to Dukhin's theory,[18] the surface conductivity of polyelectrolyte layers κ^σ is directly related to Donnan potential ψ_D as expressed by the equation

$$\kappa^\sigma = \frac{F^2 C_0 d}{RT}[D^+(e^{-\tilde{\psi}_D} - 1) + D^-(e^{\tilde{\psi}_D} - 1)] \tag{16}$$

Here, $D^\pm = u^\pm RT/F$ is the diffusion coefficient of the cation or anion and $u^\pm$ is the mobility. k_B and T are the Boltzmann constant and the absolute temperature, respectively; C_0 is the electrolyte concentration; R is the gas constant; and F is Faraday's constant. $\tilde{\psi}_D = e\psi_D/kT$ (e is the elementary charge) is the dimensionless Donnan potential, where ψ_D is the actual Donnan potential and is negative ($\psi_D \approx -0.05$ V; see Figure 4). Therefore, the second term $D^-(e^{\tilde{\psi}_D} - 1)$ of eq 16 was dropped and eq 16 is approximated as

$$\kappa^\sigma = \frac{F^2 C_0 d}{RT} D^+(e^{\tilde{\psi}_D} - 1) \tag{17}$$

The relation between Donnan potential ψ_D (or $\tilde{\psi}_D$) and fixed charge density ρ is given by

$$e^{\tilde{\psi}_D} = \frac{10^{(pH-pK)}}{2}\left(\sqrt{1 + 4\frac{|\rho|}{C_0 F}10^{(pK-pH)}} - 1\right) \tag{18}$$

where pK is the dissociation constant of acrylic acid at 25 °C. κ^σ can also be expressed by the relation with the electrical parameters of SPB and the medium (ε_{SPB}, σ_a, and κ_a):[58]

$$\omega_{MWO} = \frac{2\kappa_a}{\varepsilon_p + 2\varepsilon_a}(Du + 1) \tag{19}$$

$$Du = \kappa^\sigma / R_b \kappa_a \tag{20}$$

Here, R_b is equivalent to $R + L$ of our model, and ω_{MWO} is from the high-frequency relaxation ($\omega_{MWO} = 1/\tau_{high}$, τ_{high} is listed in Table 3). In this way, surface conductivity κ^σ, Donnan potential ψ_D, and fixed charge density ρ of the brush layer (including the charges Q which are calculated from the geometry of the brush layer) are estimated through eqs 17−20 using the parameters of the high-frequency relaxation ε_{SPB}, κ_a, and τ_{high} in Table 3, and the results are summarized in Table 4.

Table 4. Electrical Parameters of PAA Brushes in SPB Suspensions of Varying pH for 0.536% SPBs

pH	$\kappa^\sigma \times 10^8$/S	ψ_D/V	$\rho \times 10^{-5}$/C m^{-3}	$Q \times 10^{14}$/C
4.7	6.98	−0.0356	9.98	1.11
5.7	10.05	−0.0461	7.09	1.24
6.7	14.61	−0.0546	8.28	2.02
7.4	16.73	−0.0581	9.29	2.96
8.1	20.48	−0.0633	11.3	3.61
10.5	21.79	−0.0649	12.0	3.84

It is shown in Table 4 that when the fixed charge is about 1.0×10^{-14} C, the corresponding Donnan potential ψ_D is approximately −0.036 V. With the increase in pH, the charges Q increased gradually up to 3.84×10^{-14} C and the corresponding ψ_D decreased to −0.065 V, suggesting the increasing osmotic pressure in a polyelectrolyte brush.[12] The possible reason is that −COOH in the PAA chain is neutralized by OH^-, leading to the accumulation of more $-COO^-$ as the brush increases. These values of ρ (or Q) obtained here from dielectric analysis are comparable to that reported in other research by means of conductivity measurements or theoretical simulations.[19,54] Simultaneously, the diffusion rate driven by the Donnan potential ψ_D is also accelerated, resulting in a higher conductivity κ^σ. These results are in accordance with that of the PAA brush and surface-grafted poly(L-glutamic acid) brush determined by electrokinetic experiments.[19,59] In addition, the calculated κ^σ is several orders of magnitude larger than that of a polystyrene sphere, which is equivalent to the core of SPB in our work,[60] possibly attributed to the higher charge density of the brush layer. In the comparison between Table 4 and Figure 4, it is clear that the simulating values for the Donnan potential and fixed charges were completely consistent with that calculated by eqs 17−20 by using the same phase parameters. It indicates that the dielectric model we proposed in this work is appropriate for the PBS particles and supports Dukhin's theory that describes the electrokinetic characterization of polyelectrolyte brushes.

5. CONCLUSIONS AND PERSPECTIVES

In this work, we thoroughly investigated the dielectric properties of a polystyrene (PS) core-poly(acrylic acid)

DOI: 10.1021/acs.langmuir.5b01408
Langmuir 2015, 31, 8566−8576

(PAA) spherical polyelectrolyte brush (SPB) suspension. Two remarkable dielectric relaxations were first observed, which are associated with counterion diffusion and interfacial polarization between SPB and the bulk solution, respectively. We confirmed the low-frequency relaxation mechanism through the theoretical simulation based on the Poisson−Boltzmann equations. We further identified two kinds of modes of movement of counterions in the SPB suspension: the diffusion of free counterions from the bulk to the brush layer, which is responsible for the low-frequency relaxation, and the fluctuation of condensed counterions along the polyelectrolyte chains which contributes to the high-frequency relaxation. We also proposed a dielectric model to describe the high-frequency relaxation and consequently calculated the volume fraction, apparent permittivity, and conductivity of the SPB with different mass fractions and the pH of the solution. Furthermore, by combining phase parameters and the theoretical equations, we found that fixed charges and the Donnan potential increased as the pH of the solution increased, resulting in increasing degrees of dissociation and polyelectrolyte brush swelling. These results show that a typical weak acid PAA brush will provide a possibility for developing functional SPBs and their applications to more actual fields.

In addition, we determined the relaxation mechanism that verified the existing speculation about the morphology of spherical polyelectrolyte brushes. Through the calculation of the electrical parameters of SPBs and the resulting electrokinetic parameters, we described in detail the brush layer and interface properties between the brush and bulk solution at different pH values, which will enhance our understanding of the sensitivity of the PAA-type polyelectrolyte brush in solution to acidity.

We also obtained κ^{σ} for an imaginary interface by using high-frequency relaxation parameters. All of these parameters are incredibly meaningful to researchers to understand the electrical properties of polyelectrolyte brushes, especially the electrokinetic properties of ions inside polyelectrolyte brushes under different medium environments, which is also helpful in understanding the colloidal stability. Also, we estimated the fixed charges and Donnan potential in polyelectrolyte brushes.

In conclusion, our work provides new insights on dielectric behaviors of typical weak acid PAA brushes and will be helpful in the development of functional SPBs and their practical application in various fields. It is proven that dielectric studies can derive a lot of valuable information from the analysis of the dielectric spectrum of SPBs and provide the unique advantage and feasibility of obtaining quantitative information about soft particles.

■ ASSOCIATED CONTENT

Supporting Information

The dielectric measuring cell and its calibration. The Supporting Information is available free of charge on the ACS Publications website at DOI: 10.1021/acs.langmuir.5b01408.

■ AUTHOR INFORMATION

Notes

The authors declare no competing financial interest.

■ ACKNOWLEDGMENTS

We thank Prof. Kun Cao of the Department of Chemical Engineering, Zhejiang University, China, for supplying the SPB sample. This work is supported by the National Natural Scientific Foundation of China (nos. 21173025 and 21473012) and the Major Research Plan of the NSFC (no. 21233003).

■ REFERENCES

(1) Guo, X.; Weiss, A.; Ballauff, M. Synthesis of Spherical Polyelectrolyte Brushes by Photoemulsion Polymerization. *Macromolecules* **1999**, *32*, 6043−6046.
(2) Stuart, M. A. C.; Huck, W. T.; Genzer, J.; Müller, M.; Ober, C.; Stamm, M.; Sukhorukov, G. B.; Szleifer, I.; Tsukruk, V. V.; Urban, M. Emerging applications of stimuli-responsive polymer materials. *Nat. Mater.* **2010**, *9* (2), 101−113.
(3) Nabzar, L.; Duracher, D.; Elaïssari, A.; Chauveteau, G.; Pichot, C. Electrokinetic properties and colloidal stability of cationic amino-containing N-isopropylacrylamide-styrene copolymer particles bearing different shell structures. *Langmuir* **1998**, *14* (18), 5062−5069.
(4) Liu, B.-T.; Hsu, J.-P. Stability of Soft Colloidal Particles in a Salt-Free Medium. *Langmuir* **2009**, *25* (16), 9045−9050.
(5) Schneider, C.; Jusufi, A.; Farina, R.; Pincus, P.; Tirrell, M.; Ballauff, M. Stability behavior of anionic spherical polyelectrolyte brushes in the presence of La (III) counterions. *Phys. Rev. E* **2010**, *82* (1), 011401.
(6) Schneider, C.; Hanisch, M.; Wedel, B.; Jusufi, A.; Ballauff, M. Experimental study of electrostatically stabilized colloidal particles: Colloidal stability and charge reversal. *J. Colloid Interface Sci.* **2011**, *358* (1), 62−67.
(7) Lu, Y.; Mei, Y.; Schrinner, M.; Ballauff, M.; Möller, M. W.; Breu, J. In situ formation of Ag nanoparticles in spherical polyacrylic acid brushes by UV irradiation. *J. Phys. Chem. C* **2007**, *111* (21), 7676−7681.
(8) Lu, Y.; Mei, Y.; Ballauff, M.; Drechsler, M. Thermosensitive core-shell particles as carrier systems for metallic nanoparticles. *J. Phys. Chem. B* **2006**, *110* (9), 3930−3937.
(9) Jusufi, A.; Likos, C. N.; Ballauff, M. Counterion distributions and effective interactions of spherical polyelectrolyte brushes. *Colloid Polym. Sci.* **2004**, *282*, 910−917.
(10) Groenewegen, W.; Egelhaaf, S.; Lapp, A.; Van der Maarel, J. Neutron scattering estimates of the effect of charge on the micelle structure in aqueous polyelectrolyte diblock copolymer solutions. *Macromolecules* **2000**, *33* (9), 3283−3293.
(11) Guo, X.; Ballauff, A. M. Spatial Dimensions of Colloidal Polyelectrolyte Brushes As Determined by Dynamic Light Scattering. *Langmuir* **2000**, *16*, 8719−8726.
(12) Guo, X.; Ballauff, M. Spherical polyelectrolyte brushes: comparison between annealed and quenched brushes. *Phys. Rev. E: Stat. Phys., Plasmas, Fluids, Relat. Interdiscip. Top.* **2001**, *64* (5), 051406.
(13) Hoffmann, M.; Jusufi, A.; Schneider, C.; Ballauff, M. Surface potential of spherical polyelectrolyte brushes in the presence of trivalent counterions. *J. Colloid Interface Sci.* **2009**, *338* (2), 566−572.
(14) Schneider, C.; Jusufi, A.; Farina, R.; Li, F.; Pincus, P.; Tirrell, M.; Ballauff, M. Microsurface potential measurements: Repulsive forces between polyelectrolyte brushes in the presence of multivalent counterions. *Langmuir* **2008**, *24* (19), 10612−10615.
(15) Irigoyen, J.; Arekalyan, V. B.; Navoyan, Z.; Iturri, J.; Moya, S. E.; Donath, E. Spherical polyelectrolyte brushes' constant zeta potential with varying ionic strength: an electrophoretic study using a hairy layer approach. *Soft Matter* **2013**, *9* (48), 11609−11617.
(16) Ballauff, M. Polyelectrolyte brushes. *Curr. Opin. Colloid Interface Sci.* **2006**, *11*, 316−323.
(17) Wittemann, A.; Drechsler, M.; Talmon, Y.; Ballauff*, a. M. High Elongation of Polyelectrolyte Chains in the Osmotic Limit of Spherical Polyelectrolyte Brushes: A Study by Cryogenic Transmission Electron Microscopy. *J. Am. Chem. Soc.* **2005**, *127*, 9688 −9689.
(18) Dukhin, S. S.; Zimmermann, R.; Werner, C. Intrinsic charge and Donnan potentials of grafted polyelectrolyte layers determined by surface conductivity data. *J. Colloid Interface Sci.* **2004**, *274* (1), 309−318.

DOI: 10.1021/acs.langmuir.5b01408
Langmuir 2015, 31, 8566−8576

(19) Zimmermann, R.; Norde, W.; Cohen Stuart, M. A.; Werner, C. Electrokinetic characterization of poly (acrylic acid) and poly (ethylene oxide) brushes in aqueous electrolyte solutions. *Langmuir* **2005**, *21* (11), 5108−5114.
(20) Jimenez, M. L.; Delgado*, A. V.; Ahualli, S.; Hoffmann, M.; A.Witteman; Ballauff, M. Giant permittivity and dynamic mobility observed for spherical polyelectrolyte brushes. *Soft Matter* **2011**, *7*, 3758−3762.
(21) Ahualli, S.; Ballauff, M.; Arroyo, F. J.; Delgado, A. n. V.; Jiménez, M. a. L. Electrophoresis and Dielectric Dispersion of Spherical Polyelectrolyte Brushes. *Langmuir* **2012**, *28* (47), 16372−16381.
(22) Ohshima, H. Electrophoresis of soft particles. *Adv. Colloid Interface Sci.* **1995**, *62*, 189−235.
(23) Cametti, C.; Fratoddi, I.; Venditti, I. Dielectric Relaxations of Ionic Thiol-Coated Noble Metal Nanopart icles in Aqueous Solutions: Electrical Characterization of the Interface. *Langmuir* **2011**, *27*, 7084−7090.
(24) Chronopoulou, L.; A. C; Cametti, C.; Dentini, M.; Palocci, C. PLGA-based nanoparticles: Effect of chitosan in the aggregate stabilization. A dielectric relaxation spectroscopy study. *Colloids Surf., B* **2012**, *97*, 117−123.
(25) Cametti, C. Dielectric properties of soft-particles in aqueous solutions. *Soft Matter* **2011**, *7*, 5494−5506.
(26) Grosse, C. Permittivity of a suspension of charged spherical particles in electrolyte solution. 2. Influence of the surface conductivity and asymmetry of the electrolyte on the low- and high-frequency relaxations. *J. Phys. Chem.* **1988**, *92* (13), 3905−3910.
(27) Grosse, C.; Delgado, A. V. Dielectric dispersion in aqueous colloidal systems. *Curr. Opin. Colloid Interface Sci.* **2010**, *15* (3), 145−159.
(28) Schwan, H.; Schwarz, G.; Maczuk, J.; Pauly, H. On the low-frequency dielectric dispersion of colloidal particles in electrolyte solution. *J. Phys. Chem.* **1962**, *66* (12), 2626−2635.
(29) Delgado, A.; Arroyo, F.; González-Caballero, F.; Shilov, V.; Borkovskaya, Y. B. The effect of the concentration of dispersed particles on the mechanisms of low-frequency dielectric dispersion (LFDD) in colloidal suspensions. *Colloids Surf., A* **1998**, *140* (1), 139−149.
(30) O'Brien, R. W. The high-frequency dielectric dispersion of a colloid. *J. Colloid Interface Sci.* **1986**, *113* (1), 81−93.
(31) López-García, J. J.; Grosse, C.; Horno, J. Numerical study of colloidal suspensions of soft spherical particles using the network method 2. AC electrokinetic and dielectric properties. *J. Colloid Interface Sci.* **2003**, *265*, 341−350.
(32) Ge, X.; Guan, Y. X.; Chen, J.; Yao, Z.; Cao, K.; Yao, S. J. Refolding of lysozyme in vitro assisted by colloidal thermosensitive poly (N-isopropylacrylamide) brushes grafted onto the surface of uniform polystyrene cores. *J. Appl. Polym. Sci.* **2009**, *114* (2), 1270−1277.
(33) Fang, M.; Gao, J. L.; Wang, S.; Lian, Y. W.; Zhao, K. S. Dielectric Monitoring Method for the Drug Release Mechanism of Drug-loading Chitosan Microspheres. *Chin. Sci. Bull.* **2010**, *55* (13), 1246−1254.
(34) Schwan, H. P. In *Physical Techniques in Biological Research*; Nestuk, W. L., Ed.; Academic Press: New York, 1963; Vol 6, Chapter 6, pp 323−406.
(35) Cole, K. S.; Cole, R. H. Dispersion and absorption in dielectrics I. Alternating current characteristics. *J. Chem. Phys.* **1941**, *9* (4), 341−351.
(36) Hanai, T.; Imakita, T.; Koizumi, N. Analysis of dielectric relaxations of w/o emulsions in the light of theories of interfacial polarization. *Colloid Polym. Sci.* **1982**, *260* (11), 1029−1034.
(37) Serghei, A.; Tress, M.; Sangoro, J. R.; Kremer, F. Electrode polarization and charge transport at solid interfaces. *Phys. Rev. B: Condens. Matter Mater. Phys.* **2009**, *80*, 184301.
(38) Jiménez, M.; Arroyo, F.; van Turnhout, J.; Delgado, A. Analysis of the dielectric permittivity of suspensions by means of the logarithmic derivative of its real part. *J. Colloid Interface Sci.* **2002**, *249* (2), 327−335.
(39) Wübbenhorst, M.; van Turnhout, J. Analysis of complex dielectric spectra. I. One-dimensional derivative techniques and three-dimensional modelling. *J. Non-Cryst. Solids* **2002**, *305* (1), 40−49.
(40) Hanai, T. Electrical properties of emulsions. *Emulsion Sci.* **1968**, 354−477.
(41) Kuwabara, S. The forces experienced by randomly distributed parallel circular cylinders or spheres in a viscous flow at small Reynolds numbers. *J. Phys. Soc. Jpn.* **1959**, *14*, 527−532.
(42) He, K.; Zhao, K. Dielectric analysis of a nanoscale particle in an aqueous solution of low electrolyte concentration. *Langmuir* **2005**, *21* (25), 11878−11887.
(43) Zhao, K.; He, K. Dielectric relaxation of suspensions of nanoscale particles surrounded by a thick electric double layer. *Phys. Rev. B: Condens. Matter Mater. Phys.* **2006**, *74* (20), 205319.
(44) Duval, J. F. L.; Leeuwen, H. P. v. Electrokinetics of Diffuse Soft Interfaces. 1. Limit of Low Donnan Potentials. *Langmuir* **2004**, *20*, 10324−10336.
(45) Ahualli, S.; Félix, Carrique; Angel, V.; Delgado, A. C. AC Electrokinetics of Concentrated Suspensions of Soft Particles. *Langmuir* **2009**, *25*, 1986−1997.
(46) Ohshima, H. Donnan potential and surface potential of a spherical soft particle in an electrolyte solution. *J. Colloid Interface Sci.* **2008**, *323* (1), 92−97.
(47) Lide, D. R., Ed. *CRC Handbook of Chemistry and Physics*; CRC Press: Boca Raton, FL, 2003.
(48) Grosse, C.; Monica, Tirado; Witold, Pieper; Pottel, a. R. Broad Frequency Range Study of the Dielectric Properties of Suspensions of Colloidal Polystyrene Particles in Aqueous Electrolyte Solutions. *J. Colloid Interface Sci.* **1998**, *205*, 26−41.
(49) Hollingsworth, A. D.; Saville, D. A. Dielectric spectroscopy and electrophoretic mobility measurements interpreted with the standard electrokinetic model. *J. Colloid Interface Sci.* **2004**, *272*, 235−245.
(50) Li, J.; Zhao, K.; Liu, C. Dielectric relaxations of poly (acrylic acid)-graft-poly (ethylene oxide) aqueous solution: Analysis coupled with scaling approach and hydrogen-bonding complex. *Phys. Rev. E* **2013**, *87* (4), 042603. Li, J.; Zhao, K. Effect of Side-Chain on Conformation of Poly (acrylic acid) and Its Dielectric Behaviors in Aqueous Solution: Hydrophobic and Hydrogen-Bonding Interactions and Mechanism of Relaxations. *J. Phys. Chem. B* **2013**, *117* (39), 11843−11852.
(51) Vuletić, T.; Babić, S. D.; Ivek, T.; Grgičin, D.; Tomić, S.; Podgornik, R. Structure and dynamics of hyaluronic acid semidilute solutions: a dielectric spectroscopy study. *Phys. Rev. E* **2010**, *82* (1), 011922.
(52) Zimmermann, R.; Norde, W.; Stuart, M. A. C.; Werner, C. Electrokinetic Characterization of Poly(Acrylic Acid) and Poly-(Ethylene Oxide) Brushes in Aqueous Electrolyte Solutions. *Langmuir* **2005**, *21*, 5108−5114.
(53) Bordi, F. Dielectric spectroscopy and conductivity of polyelectrolyte solutions. *J. Phys.: Condens. Matter* **2004**, *16*, 1423−1463.
(54) Yezek, L. P.; van Leeuwen, H. P. An electrokinetic characterization of low charge density cross-linked polyacrylamide gels. *J. Colloid Interface Sci.* **2004**, *278* (1), 243−250.
(55) Dong, J.; Ozaki, Y.; Nakashima, K. Infrared, Raman, and near-infrared spectroscopic evidence for the coexistence of various hydrogen-bond forms in poly (acrylic acid). *Macromolecules* **1997**, *30* (4), 1111−1117.
(56) Wu, T.; Gong, P.; Szleifer, I.; Vlček, P.; Šubr, V.; Genzer, J. Behavior of surface-anchored poly (acrylic acid) brushes with grafting density gradients on solid substrates: 1. Experiment. *Macromolecules* **2007**, *40* (24), 8756−8764.
(57) Dukhin, S. S.; Zimmermann, R.; Werner, C. Surface conductivity reveals counterion condensation within grafted poly-electrolyte layers. *J. Phys. Chem. B* **2007**, *111* (5), 979−981.
(58) Delgado, Á. V., Ed. *Interfacial Electrokinetics and Electrophoresis*; Marcel Dekker: New York, 2001.
(59) Mei, Y.; Lauterbach, K.; Hoffmann, M.; Borisov, O. V.; Ballauff, M.; Jusufi, A. Collapse of Spherical Polyelectrolyte Brushes in the

DOI: 10.1021/acs.langmuir.5b01408
Langmuir 2015, 31, 8566−8576

Presence of Multivalent Counterions. *Phys. Rev. Lett.* **2006**, *97*, 158301.
(60) Jimenez, M.; Arroyo, F.; Carrique, F.; Delgado, A. Surface conductivity of colloidal particles: Experimental assessment of its contributions. *J. Colloid Interface Sci.* **2007**, *316* (2), 836−843.

DOI: 10.1021/acs.langmuir.5b01408
Langmuir 2015, 31, 8566−8576